same is probably true for the $^3A'$ state, but this process was not studied since the reaction path is completely unsymmetric and therefore more complicated to calculate. Thus one may conclude that, unless the $^1A'$ state is drastically favored with an increased accuracy of the calculation, this molecule is not stable but will dissociate into an ketone and a sulfur atom.

It seems on this basis reasonable to conclude that the strongly colored intermediates found in the photolyses of diaryloxathiiranes[2,3] at low temperature are not to be assigned to the biradical **2** (R = Ar), which leave the carbonyl *O*-sulfides as the most reasonable candidates for the experimentally observed 550-nm absorptions, as tentatively suggested previously.[3] As was the case in the CNDO/S study,[3] the agreement between the observed transition energy, 2.25 eV, and the calculated energy differences, 3.23 eV for $^1A''$ and 3.47 eV for $^1A'$, is, however, not satisfactory. The same errors as mentioned above in the thiocarbonyl *S*-oxide case are, of course, operating here, and it seems most likely that introduction of aryl groups will cause a red shift of the computed transitions, bringing the calculated and experimentally observed transitions in closer agreement.

Finally, the possible formation of the carbonyl sulfides as apparent intermediates in the photolysis will be discussed. from the previous discussion it appears that the photolysis of oxathiiranes most probably will give rise to the corresponding ketones and ^1D sulfur atoms. In the cases studied experimentally, these products are formed in a cold and rather rigid matrix (EPA or PVC); i.e., their possibility of moving apart is strongly reduced. Consequently, it is suggested that the carbonyl sulfides (**3**, R = Ar) are formed by a consecutive reaction between initially formed diaryl ketones and $S(^1D)$ atoms, a reaction which apparently proceeds without any reaction barrier (vide supra).

On the basis of the present results and the above discussions, the photolytical formation and decomposition of oxathiiranes are rationalized as visualized in the following scheme.

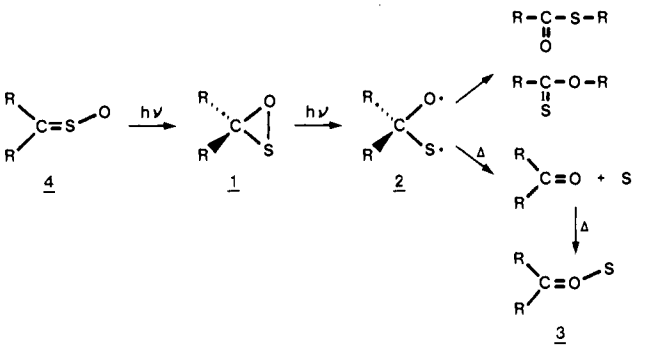

Conclusion

Oxathiiranes are generated photolytically from thioketone *S*-oxides via an excited^1 A' state. Further photolysis of the oxathiirane leads a priori to the singlet biradical **2**, which by vibrational relaxation may eliminate a singlet D sulfur atom and form the corresponding ketone and/or rearrange into the thioesters **5** and/or **6**. The experimentally observed ketone *O*-sulfides are most likely formed in the cold matrix by addition of the D sulfur atom to the ketone.

Acknowledgment. This work has been supported by a grant from the Swedish Natural Science Research Council (NFR).

Registry No. **1** (R = H), 53283-22-0; **2** (R = H), 88510-84-3; **3** (R = H), 78602-50-3; **4** (R = H), 40100-16-1.

Activation of Single-Bond Cleavage Processes on Metal Surfaces: A Comparison of Dissociative Hydrogen Adsorption with Simple Gas-Phase Exchange Reactions

T. H. Upton

Contribution from the Corporate Research—Science Laboratories, Exxon Research and Engineering Company, Annandale, New Jersey 08801. *Received May 31, 1983*

Abstract: Certain simple dissociative chemisorption processes on metal surfaces may be viewed as analogues of gas-phase bimolecular exchange reactions: AB + MM → AM + BM. We compare in detail the process of HH (or HD) dissociation on a model Ni(100) surface with both the low-barrier collinear exchange $H_2 + D \rightarrow HD + H$ reaction and the HH + DD → 2HD reaction which has a much higher barrier. We show that the state evolution which occurs during the surface reaction is entirely comparable to that in the molecular processes, and in all cases the barrier height is determined purely by the ease with which the reactants are able to meet the requirements of the Pauli principle. By analyzing the reaction on this fundamental level, we are able to avoid arguments that are based on molecule or surface orbital symmetries. The results confirm the common conjecture that low activation energies in surface reactions are in part the result of the high metal density of states and, further, demonstrate in detail how this density of states is employed to produce low barriers. We point out that, although d orbitals possess local symmetry properties that naturally satisfy certain of the Pauli principle constraints, s- and p-band metal electrons are no less capable of doing so when the density of surface states (projected onto the reaction site) is high.

I. Introduction

The concept of "reaction selection rules" is a well-known one in organic chemistry, having been the subject of a variety of theoretical studies. Efforts have ranged from the molecular-orbital-based efforts of Woodward and Hoffmann[1] and others,[2-4] to the valence-bond arguments presented originally by Goddard.[5] Each of these approaches has enjoyed considerable success, providing an understanding of a wide range of reaction phenomena in organic chemistry via relatively simple electronic structure

(1) See, for example, R. B. Woodward and R. Hoffmann, "The Conservation of Orbital Symmetry", Verlag Chemie, Weinheim, Germany, 1970, and references within.

(2) K. Fukui in "Modern Quantum Chemistry", O. Sinanoglŭ, Ed., Academic Press, New York, 1965 and references within; K. Fukui and H. Fujimoto, *Bull. Chem. Soc. Jpn.*, **41**, 1989 (1968); K. Fukui, *ibid.*, **39**, 498 (1966).

(3) H. Longuet-Higgins and E. W. Abrahamson, *J. Am. Chem. Soc.*, **87**, 2045 (1965).

(4) R. Pearson, *J. Am. Chem. Soc.*, **91**, 1252, 4957 (1969); *Acc. Chem. Res.*, **4**, 152 (1971); *Theor. Chim. Acta*, **16**, 107 (1970).

(5) (a) W. Goddard III, *J. Am. Chem. Soc.*, **92**, 7520 (1970); (b) W. Goddard III and R. C. Ladner, *ibid.*, **93**, 6750 (1971); (c) W. Goddard III, *ibid.*, **94**, 793 (1972).

0002-7863/84/1506-1561$01.50/0

arguments. Attempts to extend these ideas to organometallic chemistry, though valuable, have not proven to be nearly so comprehensive in their applicability. Perhaps not surprisingly then, applications to problems of transition metal surface chemistry have been particularly rare.[6] Here, the proper manner in which to extend the gas-phase concepts is unclear, and in fact it may be inappropriate to proceed along this route at all. Most molecular analyses make extensive use of reactant and product orbital symmetries, detailed electron counts, and Pauli principle restrictions. They take advantage of the fact that the problem is strictly a local one, the states are generally well separated, and the spin couplings well defined. The facility with which molecular bonds are broken under thermal conditions on most transition metal surfaces suggests that these criteria may well not be directly applicable to the surface problem. In theoretical analyses of surface reaction barriers, conclusions have usually been based on the electronic properties of very small metal clusters (one to five atoms). While models of this type have proven useful in studies of chemisorption, it is not clear whether conclusions about reaction probability that are based on the spin and spatial symmetries of these essentially molecular models are valid for the semiinfinite surface.

In this paper, we reconsider the question of what determines reaction barrier heights on surfaces as an electronic structure problem. We will be concerned primarily with the dissociative adsorption of molecular hydrogen on metal surfaces, taking it as a prototype for the general class of nonpolar σ-bond cleavage processes that often occur readily on these surfaces. We will draw heavily on comparisons with simple three- and four-atom gas-phase exchange processes in analyzing the evolution of states in the dissociation process. In doing so, we will avoid making direct use of spatial symmetry arguments, concentrating instead on wave-function permutational symmetries and restrictions imposed on the evolution of reactant and product electronic states by the Pauli principle. This approach to the problem is similar in spirit to that followed by Goddard[5] in studies of small-molecule problems. We make little use of orbital phases (as was done there), however, finding instead that most of the substantial differences found between molecular and surface reaction systems may be understood largely in terms of simple orthogonality constraints. The comparison with this previous work does allow us to conclude, however, that the same wave-function features that lead to high barriers in some small molecule reactions lead to very small barriers in the analogous gas-surface reactions.

II. Review of Theoretical Concepts

In this section, we will briefly review the concepts needed to understand the manner in which reactant electronic states may evolve continuously into product electronic states, paying particular attention to restrictions imposed upon this process by the Pauli principle. Certain arguments to be presented below are developed more completely elsewhere;[5,7] our goal is to illustrate only those concepts that will be relevant to the surface problem with a discussion of some simple molecular analogues.

A. Three-Electron Exchange Reaction: $H_2 + D$. Although we are not constrained by theory to do so, it is convenient to assume a collinear geometry for the reaction coordinate. It is also appropriate to assume that the entire reaction will occur on a doublet ($S = {}^1/_2$) potential energy surface. The reaction limits may thus be represented as:

$$\Psi(H_2{+}D) = {}^2\Sigma^+ = \mathcal{A}\{H_l H_c D_r(\alpha\beta\alpha - \beta\alpha\alpha)\} \quad (1a)$$

$$\Psi(H{+}HD) = {}^2\Sigma^+ = \mathcal{A}\{H_c D_r H_l(\alpha\beta\alpha - \beta\alpha\alpha)\} \quad (1b)$$

where H_l, H_c, and D_r represent orbitals (not necessarily atomic orbitals) associated with atoms H_l, H_c, and D_r, respectively. Each wave function is a proper eigenfunction of spin and corresponds to a coupling in which the first two orbitals listed are coupled into a singlet (bonding) interaction, and each of these two orbitals is predominantly triplet coupled (more precisely: ${}^3/_4$ triplet + ${}^1/_4$ singlet) to the third orbital. We depict eq 1a using standard Young tableau[8] (eq 2a) or graphically (eq 2b) as,

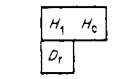

(2a)

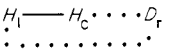

(2b)

In eq 2b, the solid line represents a singlet coupling between the orbitals connected and the sparse dotted line denotes the partial triplet coupling. The requirements that the total wave function be antisymmetric with respect to electron interchanges and have $S = {}^1/_2$ thus allows only one true "bonding" interaction in each wave function (the solid line) and necessitates two additional partial "antibonding" interactions (the dotted lines). For the separated molecule limits, these "antibonding" interactions are, of course, energetically insignificant.

At the collinear "transition state", a good approximation to the total wave function will be a superposition of the wave functions given in eq 1:

$$\Psi_\pm(TS) = (N_\pm/2)\{\Psi(H_2{+}D) \pm \Psi(H{+}HD)\} \quad \begin{matrix} +\text{ sign} & (3a) \\ -\text{ sign} & (3b) \end{matrix}$$

where $N_\pm$ is the appropriate normalization. After some rearrangement, the two wave functions become:

$$\Psi_+ = \mathcal{A}\{H_l D_r H_c(\alpha\beta\alpha - \beta\alpha\alpha)\} \quad (4a)$$

$$\Psi_- = \mathcal{A}\{H_l D_r H_c(2\alpha\alpha\beta - \alpha\beta\alpha - \beta\alpha\alpha)\} \quad (4b)$$

These correspond to the Young tableau and graphical representations:

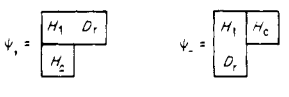

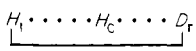

(5a)

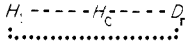

(5b)

Here, two orbitals that are triplet coupled are connected by the dense dotted lines (···), and orbitals that are partially singlet coupled are connected to each other by dashed lines (---). Ψ_- may be seen to separate the antibonding orbitals, while maximizing the overlap between partially bonding orbitals and is thus preferred over Ψ_+ where the reverse occurs. The lowest transition-state wave function is best represented by the antisymmetric superposition, Ψ_-, and, most important, the constraints of the Pauli principle (antisymmetrization) and spin disallow the simultaneous bonding between H_l–H_c and H_c–D_r that the superposition implies. Instead we have a partial bond (singlet interaction) in each case, with the penalty of an antibond (triplet interaction) between the limiting atoms H_l and D_r. This is a general result and is independent of the particular orbital shapes and symmetries involved. In fact, the orbital shapes (and locations) change significantly from those at the molecular limits in order to minimize the total energy of the system in the presence of these constraints.

To see how this happens, we examine the manner in which the orbitals of the system evolve from the separate reactant limit into the transition state. In particular, wave function 4b requires that,

(6) (a) J. Chatt and L. Duncanson, *J. Chem. Soc.*, 2939 (1953); M. Dewar, *Bull. Soc. Chim. Fr.*, **18**, C71 (1971); (b) R. Hoffmann, C. Wilker, and O. Eisenstein, *J. Am. Chem. Soc.*, **104**, 632 (1982); H. Berke and R. Hoffmann, *ibid.*, **100**, 7224 (1978); D. Thorn and R. Hoffmann, *ibid.*, **100**, 2079 (1978); N. Trong Anh, M. Elian, and R. Hofmann, *ibid.*, **100**, 110 (1978); J. Lauher, R. Hoffmann, *ibid.*, **98**, 1729 (1976); (c) C. Melius, J. Moskowitz, A. Mortola, M. Baillie, and M. Ratner, *Surf. Sci.*, **59**, 279 (1976); (d) A. van der Avoird, S. Liebman, and D. Fassaert, *Phys. Rev. B* **10**, 1230 (1974); H. Deuss and A. van der Avoird, *ibid.*, **8**, 2441 (1973); D. Fassaert and A. van der Avoird, *Surf. Sci.*, **55**, 291, 313 (1976).

(7) G. Levin and W. Goddard III, *J. Am. Chem. Soc.*, **97**, 1649 (1975).

(8) See, for example, R. Pauncz, "Spin Eigenfunctions, Construction and Use"; Plenum Press: New York, 1979.

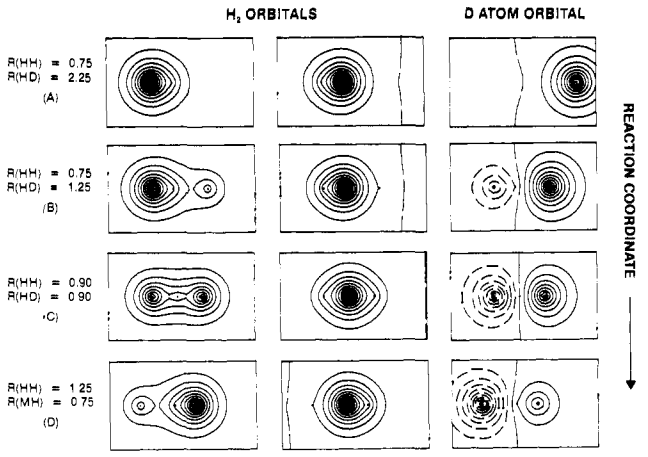

Figure 1. One-electron orbitals for the three-electron collinear exchange process in which a deuterium atom is exchanged for a hydrogen atom. Each row depicts the three optimum orbitals for a given choice of atomic coordinates. The evolution of a given orbital may be followed by moving downward in the column assigned to it. Note that orbitals on the terminal atoms have been exchanged; that is, the orbital originally on the D_r (H_l) atom evolves across to the H_l (D_r) atom. In each plot, long dashed lines are nodal planes, short dashed lines are contours of negative orbital amplitude, and solid lines are contours of positive orbital amplitude.

as the D atom approaches, the lowest energy path will be one in which the orbitals adjust to maximize bonding (and thus overlap) between the orbital originating on H_c and the terminal H_l and D_r atoms. At the same time it must minimize the repulsive triplet interactions (and thus overlap) between orbitals on the terminal atoms. It is not possible to do this effectively with atomic orbitals. In Figure 1, we show one-electron orbitals for the H_2 + D system for several values of $R(H_l$–$H_c)$ and $R(H_c$–$D_r)$. The orbitals shown were obtained in calculations in which both the one-electron orbital shapes and the spin coupling between the orbitals were optimized self-consistently (given the constraint that the total wave function have a net spin $S = {}^1/_2$).[9] Each orbital plotted has one electron, and the three orbitals in each row are the orbitals making up the total wave function for the choice of coordinates given. Thus, the evolution of each orbital through the reaction may be followed by tracing it down a given column. Substantial delocalization occurs, but for simplicity we will always label the orbitals according to the center on which they originated. As the deuterium atom approaches the H_2 molecule, the D orbital begins to take on antibonding character (Figure 1B). As the transition state is approached, the triplet coupling of H_l and D_r increases as required by eq 4b. The H orbitals are still strongly bonding, and H_c is only slightly perturbed. When the transition state is reached (Figure 1C), H_c has delocalized slightly onto both H_l and D_r (and has σ_g symmetry), but the major changes are in H_l and D_r. The D orbital has continued to become orthogonal to H_l (and now has σ_u symmetry), while the H_l orbital seeks to maintain high overlap (and thus strong bonding) with H_c (and also has σ_g symmetry). The result is a state of $^2\Sigma_u$ symmetry. It should be noted that satisfaction of the requirements that $\langle H_l|H_c\rangle \rightarrow$ maximum and $\langle H_l|D_r\rangle \rightarrow 0$ could in principle be satisfied with other choices of less delocalized orbitals (although satisfaction of the molecular symmetry requirements would require a more complicated wavefunction). There are substantial ionic contributions to the wave function at this point, however, and if we represent the total transition-state wave function in terms of atomic orbitals it would appear as,

$$\Psi_- = c_1\mathcal{A}\{H'_lD'_rH'_c(2\alpha\alpha\beta - \alpha\beta\alpha - \beta\alpha\alpha)\} + c_2\mathcal{A}\{(H'_lH'_l - D'_rD'_r)H'_c(\alpha\beta\alpha - \beta\alpha\alpha)\} \quad (6a)$$

(where the prime designates the orbitals as atomic). This may be represented equivalently with a single set of delocalized symmetry orbitals and a mixture of spin functions as,

$$\Psi_- = \mathcal{A}\{\phi_g\phi_uH_c(c_1(2\alpha\alpha\beta - \alpha\beta\alpha - \beta\alpha\alpha) + c_2(\alpha\beta\alpha - \beta\alpha\alpha))\} \quad (6b)$$

where ϕ_g ($=H_l$) $= (H'_l + D'_r)$ and ϕ_u ($=D_r$) $= (H'_l - D'_r)$ and thus the delocalized orbitals in Figure 1C are the simplest choice. The same molecular symmetry is predicted for the transition state by simple molecular orbital theory, though the evolution to this point ($H'_l \rightarrow \phi_g$ and $D'_r \rightarrow \phi_u$) is not clearly defined in that theory. The success with which the bonding objectives are met by the transition-state wave function is measured by the energy at the transition state: in these calculations it has risen only 15 kcal/mol above the reactant limit (more detailed calculations predict a value of 9.8 kcal/mol[10]). The evolution out of the transition state is shown in Figure 1D. The final state is one in which H_l and D_r have "swapped places", an apparent violation of the premise in eq 1b. That this is not a violation is more clearly seen by viewing the reaction as one in which H_c is transferred from H_l to H_r. A schematic potential curve for motion of H_c is shown in Figure 2, where the minimum energy surface evolves from the initial-state potential energy curve to the final-state curve through an avoided crossing interaction (dashed line). Changes in character of the orbitals of the type shown in Figure 1 are to be expected for such an avoided crossing.

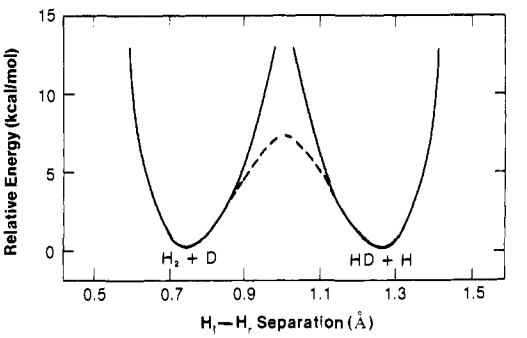

Figure 2. A schematic potential curve for collinear transfer of a H_c atom between an H_l atom and a D_r atom. The terminal H and D atoms are held fixed at a separation of 2.0 Å. The abscissa measures the separation between the H atoms. The solid lines are approximate potential curves for the isolated diatomic molecules forming limits to the transfer process. The dashed line represents an approximation to the true adiabatic potential crossing between these curves. Energy is measured relative to the diatomic potential minima.

B. Four-Electron Exchange Reaction: $H_2 + D_2$. The same type of analysis may be applied to the four-electron reaction, with rather different results. For simplicity, we assume a coplanar arrangement of the atoms, but use an asymmetric "parallelogram" interaction geometry as depicted in eq 8.[11] We write the reactant and product wave functions as (using C_{2h} symmetry):

$$\Psi(H_2{+}D_2) = {}^1A_{1g} = \mathcal{A}\{H_lH_rD_lD_r(\alpha\beta\alpha\beta - \beta\alpha\alpha\beta - \alpha\beta\beta\alpha + \beta\alpha\beta\alpha)\} \quad (7a)$$

$$\Psi(HD{+}HD) = {}^1A_{1g} = \mathcal{A}\{H_lD_lH_rD_r(\alpha\beta\alpha\beta - \beta\alpha\alpha\beta - \alpha\beta\beta\alpha + \beta\alpha\beta\alpha)\} \quad (7b)$$

and for the transition state (in which all neighboring bond distances are equal):

$$\Psi_\pm(TS) = (N/2)\{\Psi(H_2{+}D_2) + \Psi(HD{+}HD)\} \quad (7c)$$

While undoubtedly not the true saddle point in the reaction, this

(9) A computational procedure developed by F. Bobrowitz, based on R. Ladner and W. Goddard III, *J. Chem. Phys.*, **51**, 1073 (1969), and F. Bobrowitz, Ph. D. Thesis, California Institute of Technology, 1974.

(10) B. Liu, *J. Chem. Phys.*, **58**, 1925 (1973).

(11) This geometry is chose to minimize the influence of ionic contributions, which as noted in the discussion of eq 6, lead to highly delocalized orbitals at the saddle point. The "parallelogram" geometry chosen here will minimize the overlap between the D_l and D_r orbitals (see eq 8c), and lead to their localization in the transition state. This is done purely to facilitate the discussion by maximizing the similarity between the three-atom and four-atom (electron) processes.

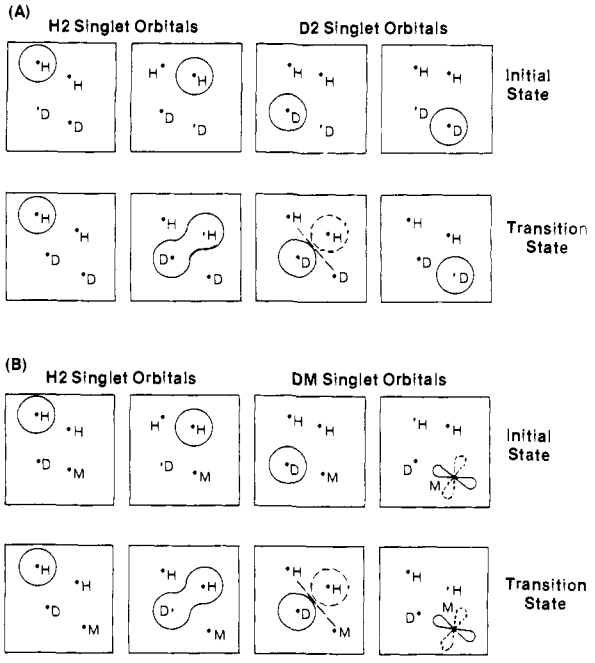

Figure 3. Sketches of the one-electron orbitals that occur in the four-electron coplanar exchange process. Each row in the figure depicts the four orbitals that are involved in the process for a particular choice of coordinates. In Figure 3A, the first row represents the H–H and D–D reactants, while the second row shows the orbitals at the approximate position of a saddle point in the process (columns are related as in Figure 1). In Figure 3B, one of the D atoms has been replace by a metal. A single contour is shown for each orbital, with phases as defined in Figure 1.

geometry allows us the simplification of assuming that H_l and D_r do not overlap at any point in the reaction. Treatment of more realistic symmetric transition-state geometries leads to the same conclusions, though the more complex orbital shapes that occur in these cases necessarily complicate the analysis.[11] As for the three-electron case, the two possible transition-state wave functions present tradeoffs between bonding and antibonding interactions, and the lowest energy state may be identified by inspection. We depict in terms of Young tableau and graphical representations the lowest energy wave functions 7a–c as:

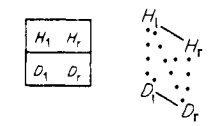
(8a)

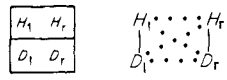
(8b)

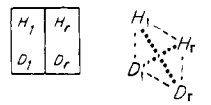
(8c)

As in the three-electron case, the approach toward the transition state requires that the spin coupling between H_l and D_r as well as H_r and D_l take on greater triplet character. This requires no changes for H_l and D_r as they are noninteracting by design.[11] The H_r and D_l pair must respond much as the terminal atoms in the H_2 + D case; however, H_r will seek to maximize its overlap with H_l and D_r in the transition state to retain bonding character, and minimize its overlap with D_l (as required be eq 8c. To achieve this, H_r delocalizes across to D_l in a bonding manner, while D_l forms an antibonding orbital between H_r and D_l. This process is shown schematically in Figure 3A (the figure is constructed in the same way as Figure 1). By symmetry, the new D_l antibonding orbital cannot overlap any of the other orbitals in the system. This has a large negative energetic effect, as overlap between D_l and both H_l and D_r is necessary to strengthen the bonding interactions between these orbitals that are defined in eq 8c. In effect, the energy of a full bond is lost. That this is true may be seen by expanding approximately the energy of the self-consistent transition-state wave function shown in Figure 3A in terms of atomic orbitals to obtain,

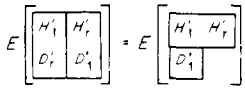
(9)

that is, the final energy is approximately that of an H_2D unit (compare with eq 2a) and a separate D atom. From an analysis of this type, one may immediately speculate that the size of the barrier in reactions of this type should be highly dependent on the local symmetries of the orbitals involved. For example, consider replacing the D_r atom with a transition metal complex such as $TiCl_3$, in the hypothetical reaction:

$$TiCl_3\text{–}D + H_2 \rightarrow TiCl_3\text{–}H + HD \qquad (10)$$

Schematically, the exchange reaction appears as shown in Figure 3B (ignoring ligand orbitals), where the metal presence is indicated by a 3d orbital, bonding initially to the D atom. Here, the "broken-bond" interaction that produced the high barrier in the previous example is reduced. Delocalization of D and H_r occurs here too (compare columns 2 and 3 in Figures 3a and 3b), but the antibonding D orbital (column 3) is able to retain significant overlap with the M 3d orbital in the transition state. All the desired overlaps appear in this transition state, and thus very little energy is lost on evolving from reactants to this point. This picture is oversimplified, yet detailed calculations on systems of this type verify the important features.[12a,b] It is easily extended without modification to reactions that involve π-bond cleavage rather than the σ-bond reactions discussed here. As an example, the ease with which olefin insertion (eq 11) and β-elimination (eq 12) processes occur for a number of metals is expected, and well-documented:[12]

$$(\pi\text{-}C_2H_4)MCH_3L_n \leftrightarrow MC_3H_7L_n \qquad (11)$$

$$MC_2H_5L_n \rightarrow MHL_n + C_2H_4 \qquad (12)$$

In principle, local electronic excitation of the H_2–D_2 system (e.g., 1s → 3d) would produce the same result were it not for the fact that the appropriate atomic states require a greater excitation energy than the experimental barrier. The essential point, as it relates to this study, is that the barrier height in a reaction of this general type is necessarily tied to the degree with which the electronic structure of the system either possesses orbitals which can accomodate the constraints of the Pauli principle without disruption, or can access orbitals with these properties (through electronic excitation). In the next sections, we will discuss a series of calculations which suggest that many metals (particularly transition metals), because they possess a high density of states near the Fermi surface, are capable of satisfying either of these two criteria in reactions of this type that occur at the surface.

III. Electronic Structure of H_2 Dissociation on Ni

The review of the previous section was essential to bring together those concepts needed to address the question of how we may break the same H–H (or H–D bond) and form H–metal bonds. We are particularly interested in the role played by the metal states in making this process energetically more favorable than analogous small-molecule symmetric hydrogen additions. In this section we present the results of calculations carried out to gain qualitative insight into this process as it occurs on a model nickel (100) surface. We will be concerned primarily with the role played by 4s–p "conduction-band" electrons in this reaction, in order to simplify both the computations and the analysis. The additional contribution due to 3d electrons, because it requires far greater

(12) (a) T. H. Upton and A. K. Rappe, to be submitted for publication; (b) M. Steigerwald, private communication; (c) see, for example, J. Collman and L. Hegedus, "Principles and Applications of Organotransition metal Chemistry", University Books, Mill Valley, Calif., 1980.

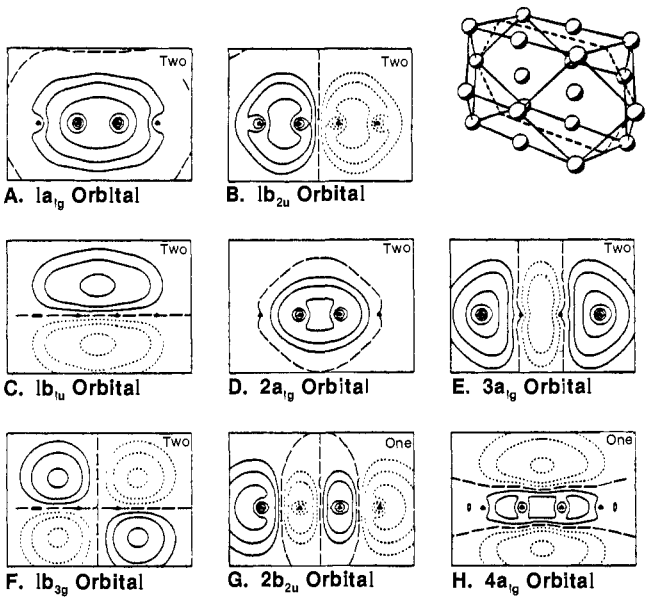

Figure 4. The 20-atom Ni cluster used in the calculations. The atoms are located in bulk fcc Ni lattice positions, and assume the geometry shown at upper right. The (001) direction points upward in the figure. The ground-state "conduction band" orbitals are shown, with orbital occupancy as shown at the upper right in each plot. The highest occupied orbitals are labeled G and H. The plotting plane is the (110) plane shown by the dashed band on the cluster. The phases and nodes in the orbital plots are as defined in Figure 1.

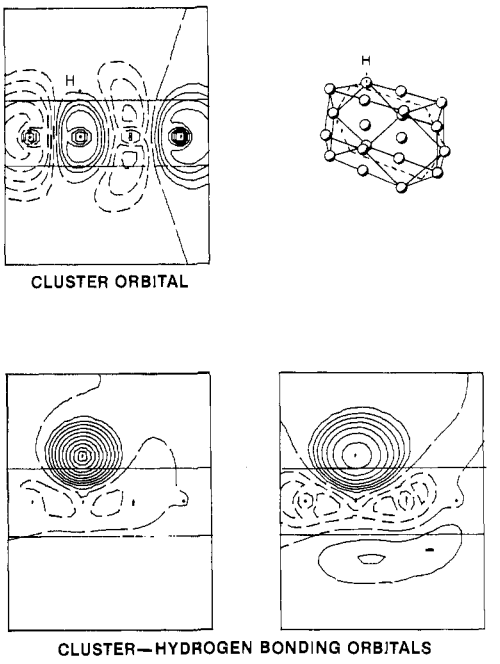

Figure 5. The three orbitals interacting to produce the Ni–H bond at a fourfold site on the (001) surface. The remaining cluster orbitals (not shown) were only slightly perturbed. The plotting plane is the same as used in Figure 4, and the H atom lies 0.5 Å above the fourfold site. The solid horizontal lines show the positions of the surface planes.

computational effort to accurately assess and obscures the important contribution of the conduction band, will be dealt with only in qualitative terms in this initial study. For reference purposes, we first briefly summarize calculations carried out to characterize both the model cluster used to represent the nickel surface, and the interaction of H atoms with the (100) "face" of this cluster.

A. The Ni_{20} Cluster. The Ni_{20} cluster model for the bulk metal has been used extensively in studies of both atomic[13] and molecular[14] chemisorption on the low index faces of Ni. In all calculations, pseudopotentials were used to represent the coulomb and exchange fields of the metal core electrons.[15] Calculations have been carried out considering H[13] and CO[16] chemisorption, in which atoms nearest the high-symmetry binding sites were allowed full variational freedom in the 4s and 3d electrons (i.e., all such orbitals were self-consistently optimized using a variationally constrained and energetically bounded procedure), while surrounding atoms were allowed freedom only in the 4s electrons (the $3d^9$ shell was frozen in an atomic configuration and included in the pseudopotential). Additional calculations were carried out in which the $3d^9$ shell was frozen in this way for all metal atoms. For stable chemisorption sites (particularly for high-symmetry H adsorption sites), the results were found to differ by 10% or less in calculated observable properties. All calculations reported here have been carried out using this approximation, and at least a concomitant degree of uncertainty is assumed.[17]

The cluster is shown in Figure 4. The atoms are arranged with an fcc structure and lattice spacings appropriate for bulk Ni. The one-electron "conduction band" states calculated for the cluster are found to be fully delocalized over the cluster. Orbitals for the ground state of the cluster, a triplet state, exhibit this property, and are also shown in Figure 4. The orbitals, labeled A–H in the figure, increase essentially monotonically in orbital energy (i.e., as labeled). Attempts to determine the importance of electron correlation effects via both self-consistent generalized valence bond (GVB)[18] and configuration interaction (CI) calculations have yielded values of the order of 0.2 eV per electron, consistent with an interpretation of these states as being only weakly intereacting. A total of 14 many-electron excited states have been found within 2 eV of the ground state with exchange couplings between high-lying half-filled orbitals characterized by exchange integrals of order 0.1 to 0.2 eV, again consistent with the weakly coupled view and suggestive of a highly polarizable electron density. The ionization potential ("work function") for this cluster has been found to be 5.9 eV, close to the experimental value of 5.2 eV. The electron affinity, on the other hand, is considerably smaller, at 2.5 eV. The reason for this behavior are discussed elsewhere.[19]

B. Atomic Hydrogen Chemisorption. Carrying out calculations to consider the interaction of an H atom with the cluster reveals a feature that is of primary importance for the purpose of this study. As the H atom approaches a high-symmetry site, such as a fourfold site on a (001) face, the cluster orbitals respond and ultimately a bond is formed. It is the response that is significant: only the highest occupied states of the cluster possessing amplitude at the surface are substantively affected by the H-atom presence. The bonding orbital that is formed is localized about the H atom and has an orbital energy much larger than the unperturbed cluster orbital. The other occupied orbitals undergo only minor changes in shape and energy as a result of the perturbation.[13] They are of secondary importance to the adsorption process, primarily providing a coulomb and exchange field in which the adsorption "reaction" occurs. These results imply that we need only concentrate on the details of the interaction between these high-lying states and the adsorbate states in order to understand the essential features of the adsorption process.

(13) T. Upton and W. Goddard III in "Chemistry and Physics of Solid Surfaces", Vol. 3, T. Vanselow and W. England, Eds., CRC Press, Boca Raton, Fla., 1982, p 127; *Phys. Rev. Lett.*, **42**, 472 (1979).
(14) T. Upton, *J. Vac. Sci. Technol.*, **20**, 527 (1982).
(15) Using the method of C. Melius, B. Olafson, and W. Goddard III, *Chem. Phys. Lett.*, **28**, 457 (1974), as modified by M. Sollenberger, M. S. Thesis, California Institute of Technology, 1975.
(16) T. Upton, unpublished results.
(17) Basis sets and effective potentials (pseudopotentials) used for the Ni atoms are tabulated in ref 13. For the H atom, the 4s Gaussian basis from T. Dunning and P. Hay, "Modern Theoretical Chemistry", Vol. 3, H. Schaefer, Ed., Plenum Press, New York, 1977, was scaled by a factor of 1.2 and augmented with a single 2p Cartesian Gaussian set with an exponent of 1.0.
(18) The GVB formalism is detailed by Bobrowitz and Goddard, ref 17.
(19) C. Melius, T. Upton, and W. Goddard III, *Solid State Commun.*, **28**, 501 (1978).

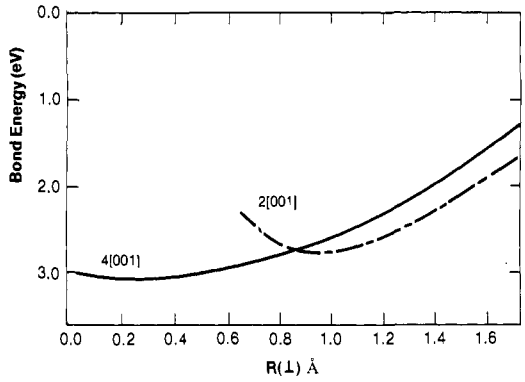

Figure 6. Potential energy curves for the interaction of an H atom with high-symmetry sites of the Ni(001) surface.

The two highest occupied orbitals of the cluster ground state (Figure 4G,H) are triplet coupled, and each possesses significant density on the (001) face. An approaching H atom interacts primarily with these two orbitals, producing a composite state with $S = {}^1/_2$ (a doublet). The response of the two cluster orbitals to H-atom approach at a fourfold site on the (100) surface is shown in Figure 5. The bonding orbitals still show remnants of their initial state character: an isolated H orbital and the cluster orbital shown in Figure 4H. The remaining orbital shown in Figure 5 is only slightly perturbed from its initial state character (Figure 4G). Formally, the process of bond formation is similar to the H_2 + D reaction depicted in eq 1–3 above, with wave-function evolution occurring as (half-filled states only):

$$^2(^3\mathrm{M} + {}^2\mathrm{H}) \rightarrow {}^2\mathrm{MH}$$

where the superscripts indicate the spin of the reactants and products. This is more completely written as,

$$\mathcal{A}\{M_1M_2H(2\alpha\alpha\beta - \alpha\beta\alpha - \beta\alpha\alpha)\} \rightarrow \mathcal{A}\{M_1HM_2(\alpha\beta\alpha - \beta\alpha\alpha)\} \quad (13a)$$

where we begin with a wave function in which the metal orbitals are coupled into $S = 1$ (triplet) and the H orbital lowers this to $S = {}^1/_2$ (doublet). In the final state H and M_1 (Figure 4H) form a bond (S = 0) and the remaining metal orbital M_2 (Figure 4G) raises this to $S = {}^1/_2$. In terms of Young tableau or a graphical representation, this becomes:

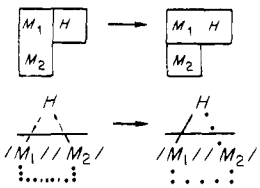

This may be written instead as a mixture of initial states which evolve as the H atom approaches,

$$\mathcal{A}\{M_1HM_2(c_1(\alpha\beta\alpha - \beta\alpha\alpha) - c_2(2\alpha\alpha\beta - \alpha\beta\alpha - \beta\alpha\alpha))\} \rightarrow \mathcal{A}\{M_1HM_2(\alpha\beta\alpha - \beta\alpha\alpha)\} \quad (13b)$$

where in (13b) it is apparent that the chemisorption process may be thought of as the evolution of $c_2 \rightarrow 0$ (at $R(\mathrm{MH}) = \infty$, $c_1 = 3^{1/2}/2$, and $c_2 = {}^1/_2$). At each stage in the calculations, the total wave function was optimized with respect to both space and spin parts of the wave function, and thus the gradual change in spin coupling is self-consistently incorporated into the shapes of the orbitals. The potential curves that result when this evolution is carried out at both twofold (bridge) and fourfold sites are shown in Figure 6. The fourfold site is found to have the larger binding energy, in agreement with current experimental interpretations,[20] and the calculated adsorption enthalpy of 3.0 eV and vibrational frequency of 592 cm^{-1} are in good agreement with well-known experimental values.[20,21] At a distance far from the surface, the

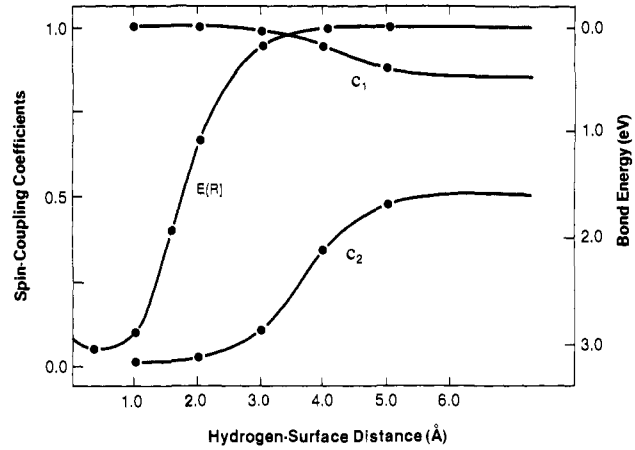

Figure 7. The evolution of coefficients from eq 13 are plotted with the potential curve that results from this state evolution. The potential energy curve is plotted according to the scale at right; the coefficients are plotted according to the left scale. The curves plotted were fit to the data points shown.

H-atom orbital begins to interact attractively with cluster state M_1. The coefficients c_1 and c_2 are plotted in Figure 7 for an H-atom approach to the fourfold site, where it may be seen that the evolution of the spin functions is essentially complete at a very long distance from the surface, while the bond strength is still less than 1.0 eV. This unusual behavior is significant; it suggests that spin-state mixing can occur in molecule–surface interactions at distances where almost no energetic interaction is present, and where details of the possible final chemisorbed states are unimportant.

C. HD Approach along Molecular Axis. To maintain the analogy with molecular processes, we consider the approach of an HD molecule toward the surface with its molecular axis directed along the surface normal above a fourfold site on Ni(001) (with the D atom closest to the surface). This contrived geometry was chosen so as to capitalize on the simplicity of the resulting interactions. We consider the stretching and cleaving of the H–D bond for various distances of the molecule above the surface. As in atomic hydrogen chemisorption, calculations reveal that only the highest occupied cluster states participate substantively in the dissociative adsorption process. If we force the highest two cluster orbitals to be singlet-coupled (this singlet state is 2 kcal/mol above the triplet cluster ground state in these calculations), then we may for illustrative purposes approximate the saddle point in the reaction by analogy with the H_2 + D_2 reaction as,

$$\Psi_{TS} = N_+/2\mathcal{A}\{\Psi(HD+M_1M_2) + \Psi(M_1D+M_2H)\} = \mathcal{A}\{M_1HM_2D(2\alpha\alpha\beta\beta + 2\beta\beta\alpha\alpha - \alpha\beta\alpha\beta - \beta\alpha\beta\alpha - \alpha\beta\beta\alpha - \beta\alpha\alpha\beta)\} \quad (14a)$$

Strictly speaking, the absence of symmetry in the problem prevents us from knowing whether this is truly an accurate representation of the saddle-point wave function (a simple 1:1 superposition of initial and final states likely does not provide a quantitative representation), but for our qualitative purposes eq 14 is adequate. Graphically, and in terms of tableau, it becomes,

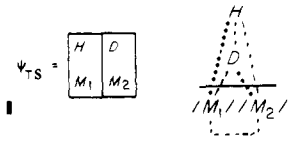

(14b)

From earlier discussion of the molecular reaction, it is apparent that the orbital initially associated with the D atom will seek to maximize overlap and bonding with the H-atom orbital and one of the cluster orbitals (M_1 above and, specifically for Ni_{20}; Figure 4H), and become orthogonal to the other (M_2 or Figure 4G) to

(20) S. Andersson, *Chem. Phys. Lett.*, **55**, 185 (1978).

(21) J. Lapujoulade and K. Neil, *Surf. Sci.*, **35**, 288 (1973).

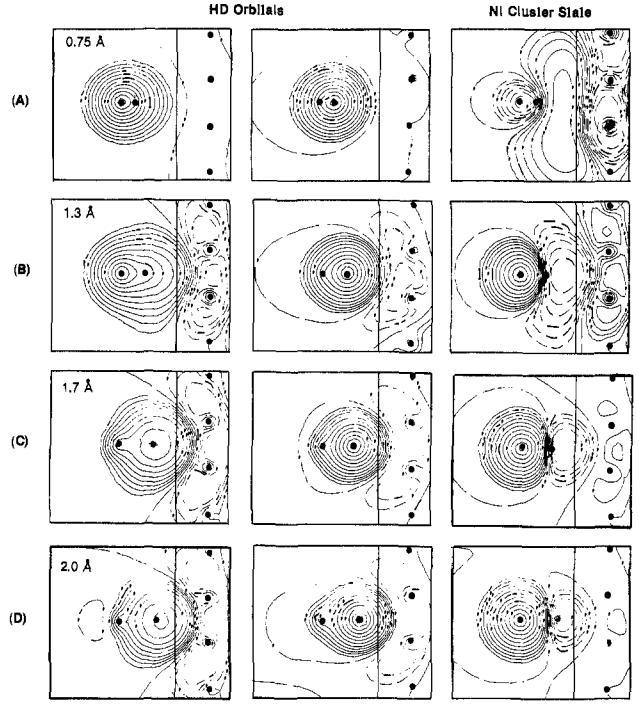

Figure 8. One-electron orbitals for the interaction of an HD molecule with a fourfold site on the Ni(001) surface. The HD molecular axis is normal to the surface above the fourfold site in all plots. The H atom is fixed at 3.0 Å above the surface, and the HD separation used to produce each row of plots is shown at the upper left in each row. The "surface" is at right in each plot, and the plotting plane chosen is the same as in previous figures. The first layer of metal atoms does not lie in the plotting plane (see Figure 4), and its position is indicated by the dark solid line in each plot.

minimize triplet repulsions. The H atom will seek to do the reverse: maximize interactions with M_2 (and D) and minimize overlap with M_1. An energetic barrier will occur that reflects the ability of the cluster and HD states to achieve these relationships (i.e., the degree of excitation required to achieve them, or the degree of "broken bondedness" that results from failure). Under optimum conditions, the transition state will reflect the four partial bonds shown in eq 14b, but will be dominated by the partial HD and DM_1 bonds, which are the strongest initial and final-state bonds. Because it is constrained to have a longer bond length, the HM_2 bond will contribute less to the energetics at all points in the reaction, and will contribute less to the evolution of the orbital shapes. We will concentrate on the interactions involving H and D and surface state M_1. To examine this one-electron-state evolution in detail, it is helpful to compare features of Figures 1 with Figure 8 where orbitals for the cluster process of dissociating the HD molecule are shown. In Figure 8A, the initial H and D orbitals are shown, along with the highest cluster orbital (originally Figure 4H, but now slightly perturbed by the presence of the HD molecule). In Figure 8B,C, the H atom remains fixed, but the D atom is moved to approximately the transition-state position. The D orbital (center column in Figure 8) remains largely unchanged (as does H_c in Figure 1). It stays highly localized on the D atom. Similarly, the orbital, which begins as H in Figure 8A (left column), progressively delocalizes onto the D atom and the surface (compare with H_1 in Figure 1). The perturbation of the cluster orbital is also extensive, and its behavior is analogous to the D_r orbital in Figure 1. This orbital evolves across the H and D atoms, becoming orthogonal to H in order to minimize the triplet interaction with the H orbital required by eq 14. The final state, as shown in Figure 8D, shows that two orbitals (originally H and M_1) have effectively "swapped" positions, resulting in the formation of an Ni–D bond (orbitals in the left two columns of Figure 8D; compare with Figure 5) and an orbital (right column) now localized on the H atom. In fact, this orbital represents half of a weak Ni–H bond to the cluster state M_2 (not shown) which

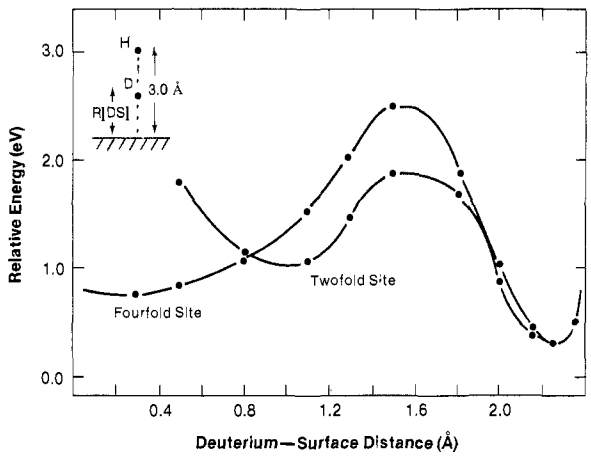

Figure 9. Potential energy curves for the dissociation of an HD molecule above different sites on the Ni (001) surface. The molecular axis is oriented normal to the surface above the twofold (bridge) or fourfold sites. The H atom is held fixed at 3.0 Å above the surface, and the total energy is plotted as a function of the distance of the D atom above each site. The curves plotted were fitted to the data points shown.

has complex nodal structure to avoid the Ni–D bond. As was noted for the molecular reactions, this swapping of orbital character is a manifestation of an avoided crossing of the unperturbed initial and final states. The most important feature of this overall process is that these complex readjustments are able to occur with relatively little cost in energy. We have illustrated the process using Figure 8 as if it were a three-electron reaction, because of the weak interactions involving the fourth orbital (electron). It is important to remember that the process is, in fact, formally more analogous to the $H_2 + D_2$ process, and that a high barrier might have been expected. Just as in the d-orbital process illustrated in Figure 3B, the nodal structure needed to minimize repulsions in the transition state is easy to develop into the wave function while maintaining bonding character. In contrast to the situation in Figure 3B, the ground-state cluster orbitals do not possess this local symmetry, but because of the high density of low-lying cluster states the excitation necessary to achieve it is minimal. This is likely to be true in general for surface conduction band states, and thus we believe that it is a primary feature needed to explain the relatively common occurrence of low barriers in simple cleavage processes on metal surfaces.

In Figure 9, potential curves are shown for a process in which the H atom is held fixed at 3.0 Å above the surface and the D atom is moved along the normal toward both the twofold (bridge) and fourfold sites. The energy is measured with respect to an isolated HD molecule and the surface. The curves are very similar for HD separations up to about 1.2 Å (D-surface distances greater than 1.8 Å), indicating the loss of specific site character at these distances. The barrier for HD cleavage appears at approximately the same position in each case (R(DM) $\sim$ 1.6). Differences in height of the barriers reflect the fact that longer DM bonds are formed at the bridge site (R_e(DM) $\sim$ 1.0 Å (twofold) vs. R_e(DM) $\sim$ 0.3 Å (fourfold)). For this site, the final state begins to contribute energetically to the wave function while the D atom is further from the surface. Beyond the barriers, the location and depth of the local minima in each case correspond closely to the positions normally assumed by isolated chemisorbed H or D atoms (see above). The long (3.0 Å) Ni–H bonds that form after the HD bond is broken (i.e., for R(DM) < 1.6 Å) contribute almost nothing to the total energy (see Figure 7).

In Figure 10, a more complete potential surface is shown, illustrating the energetic change associated with variations in both H and D positions above the fourfold site. Data from detailed calculations are represented by points in the plot; the remainder of the surface was generated by fitting cubic splines in two dimensions. The data used to create Figure 9 are taken from the horizontal boundary at the top of Figure 10. It is apparent here that the path to dissociation represented by Figure 9 is not the most favorable. Following the minimum-energy path in Figure

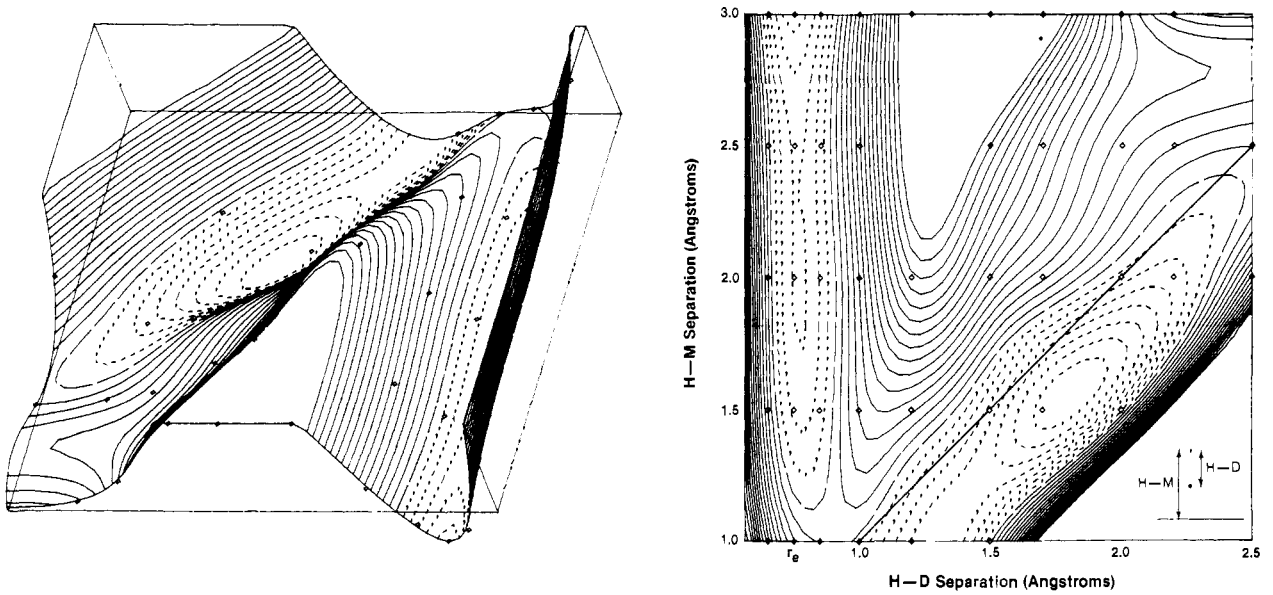

Figure 10. A potential energy surface for the dissociation process depicted in Figures 8 and 9. The zero of energy is denoted by the long dashed contour and is set to the energy of the saddle point. The contour spacing is approximately 3 kcal/mol (0.005 au). Short dashed contours are below the saddle point, solid contours above it. The straight diagonal line marks the position of the surface in these coordinates.

10 from the "reactants", there is a slight elongation of the HD bond and an increase in energy as the electrons in the strong HD bond encounter Pauli repulsions with the surface states. Stretching of the HD bond becomes increasingly favorable as the H atom is brought toward the surface until at R(HM) = 1.5 Å, where the energy has risen about 10 kcal/mol with respect to isolated HD, there is only an additional 8-kcal/mol barrier to bond cleavage from the equilibrium HD separation (0.8 Å). The solid diagonal line marked in the figure represents the position of the first plane of metal atoms within this coordinate system. At all points to the right of this line, the D atom has penetrated the surface. The line coincides closely with the energy contour defining the position of the saddle point found for this process (the long dashed line in the figure). Thus, carrying out the reaction adiabatically along the minimum energy trajectory on this surface necessarily leads to the local minimum at the right of the surface layer line in Figure 10 in which the D atom was slightly below the metal atom surface layer (about 0.3 Å), and the H atom was also bound to the surface at a distance of about 1.5 Å above the fourfold site. This choice of coordinates reflects the system's attempts to maximize the strength of both the Ni–H and Ni–D bonds and minimize the interaction between these two bonds (the final state is analogous to that depicted in eq 8b where the interaction between bonds is predominantly of triplet character and thus repulsive). We emphasize here, however, that this approach geometry is highly artificial and that in all probability this local minimum would be unstable with respect to migration of the H atom to another site on the surface.

D. HD Axis Parallel to Metal Surface. The equations used to represent dissociation in the previous section (eq 14a,b) are equally appropriate here since they are independent of spatial symmetry or coordinate details. As indicated graphically in eq 14b, each orbital will seek to maximize the stabilizing effect of two partial bonding interactions while minimizing the destabilizing effect of a third triplet interaction. In this case, both H- and D-atom orbitals may overlap strongly with each other or with the appropriate surface states at all times as the molecule is brought closer to the surface and the bond is stretched. A close analogy is maintained with the processes depicted in Figure 3. While obviously a low barrier is not guaranteed, the results presented in the previous section suggest that the surface states should be able to achieve the relationships needed for a low barrier via low-energy excitations. The dissocative adsorption process is depicted using orbital plots in Figure 11. As in the previous cluster calculations, only the highest two half-filled cluster states (Figure 4G,H) were involved in the adsorption process to any significant extent. The first row of plots (Figure 11A) shows these two orbitals as the two plots on the left (labeled M_1 and M_2), while the two orbitals forming the HD bond are shown on the right (labeled D and H). Comparison with Figure 4 shows that one of the orbitals, M_2, is only slightly perturbed (compare Figure 4G with Figure 11A, column 1). Orbital M_1 (originally Figure 4H), strongly overlaps the HD bond and reacts to eliminate this overlap. This repulsive interaction raises the energy over the separate HD and Ni limit by about 6 kcal/mol and occurs while the HD molecule is still far from the surface (2.0 Å). In Figure 11B, the HD molecule has been moved closer to the surface (1.0 Å) and the bond has been stretched to 1.05 Å. The energy has risen still further by about 9 kcal/mol at this point. The evolution of the individual one-electron states may be followed by moving downward in each column in the figure. Two significant changes have occurred in Figure 11B. The cluster orbital M_1 has formed antibonding character on the HD centers in order to remain orthogonal to orbitals associated with those centers. The H orbital (column 3) is no longer the mirror image of D in column 4 as it was in Figure 11A, but is now more diffuse and forming greater amplitude on the D atom and on the surface. The evolution of the orbitals in Figures 11A and 11B should be compared with the evolution toward a saddle point shown in Figure 3A. The change in H in Figure 11 (delocalization across D and the Ni atoms) is analogous to the H_r change in figure 3A (second column). The change in M_1 (formation of antibonding character) in analogous to D_1 in Figure 3a (column 3). The remaining orbitals in both cases are only slightly perturbed. In fact, as is discussed below, the coordinates represented in Figure 11B are approximately those of the saddle point for this process as well. As the bond is stretched (Figure 11C), these changes continue. The H orbital has continued to move over onto the D atom and has started to build more amplitude on the Ni atoms. The D orbital remains localized on the D atom. The M_1 orbital has become more localized on the H atom and is, in fact, almost the mirror image of D. At this position, the saddle point has been passed, and the formation of individual H–Ni and D–Ni bonds has begun. The energy has dropped about 2 kcal/mol from Figure 11B. It drops an additional 13 kcal/mol on going to Figure 11D, where the formation of the final-state bonds is essentially complete. Both atoms are now bound within the same fourfold hollow, and the diffuse bonds still interact repulsively. Centering both atoms on adjacent fourfold hollows lowers the energy monotonically by about 22 kcal/mol to a true final-state energetic minimum.

A potential energy surface for the process in which both the HD separation and distance above the surface (h) are varied is

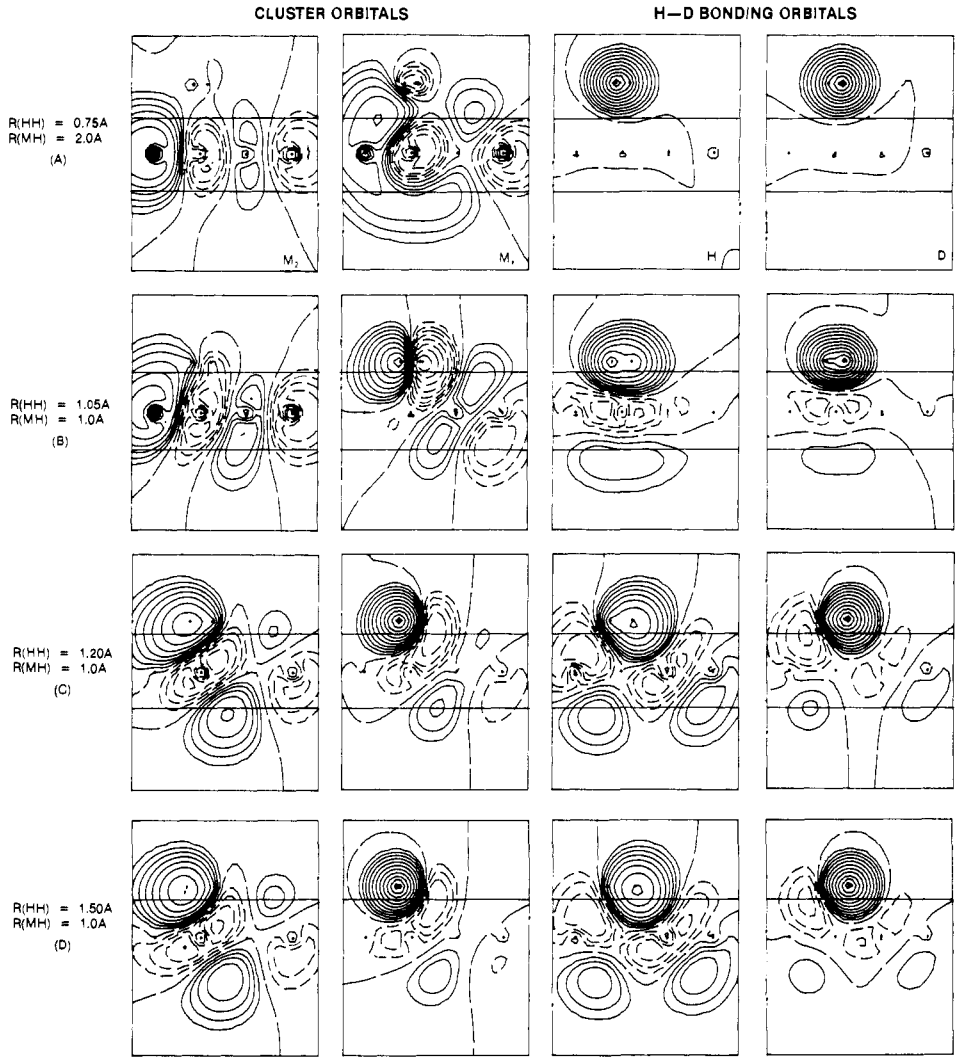

Figure 11. Evolution of one-electron orbitals in the dissociation of an HD molecule with its axis held parallel to the metal surface. As the bond is stretched, the HD center of mass remains centered over the fourfold hollow site. Each row depicts the four orbitals involved in the process for the coordinates shown; the evolution of a given orbital, may be traced down the column. The plotting plane, surface lines, and phases are as defined in Figure 5.

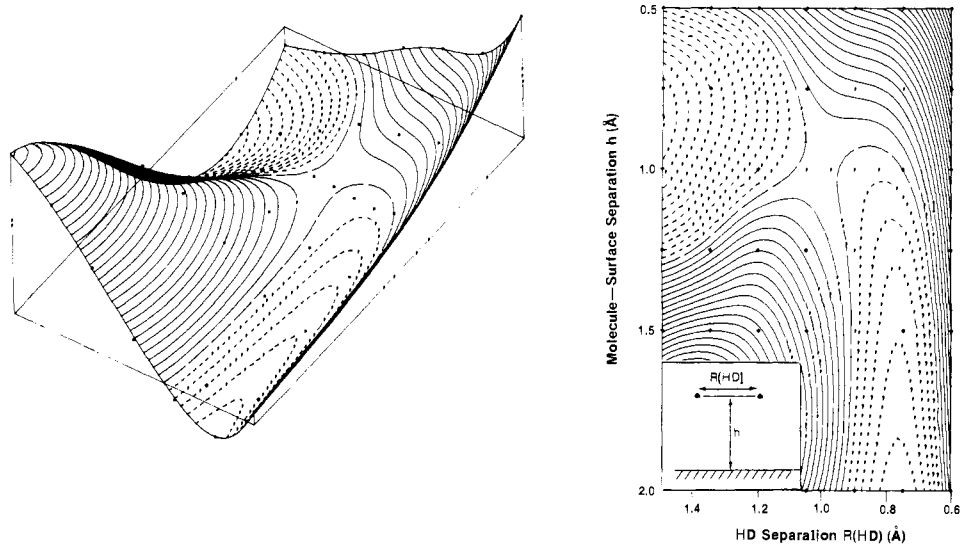

Figure 12. A potential energy surface for the dissociation process depicted in Figure 11. The zero of energy is set at the same position as in Figure 10 for comparison, and is denoted by the long dashed line. Short dashed contours are energies less than this, while solid contours are at greater energies. Contours are separated by approximately 3 kcal/mol.

shown in Figure 12. As the HD molecule is brought toward the surface, the HD equilibrium distance (defined as the point at which $(dE/dR(HD))_h = 0$ for various values of h) increases, and the force constant for HD stretching ($(d^2E/dR(HD)^2)_h$) decreases. A broad saddle point appears, centered at about $h = 1.0$ Å, beyond which appears the minimum associated with formation of bonds

between the H and D atoms and the surface. Unlike the approach geometry discussed in the last section, both atoms remain above the surface at all points in the process. Perhaps surprisingly, the barrier in Figure 10 is lower than that of Figure 12 by about 6 kcal/mol in these calculations (10 vs. 16 kcal/mol relative to isolated HD and Ni).

IV. Discussion

While we have dealt in detail with only a small number of possible reactions, there are essentially three conclusions to be conveyed which should be quite general.

(1) The unifying feature determining barrier heights, and thus reaction probabilities in both molecule–molecule interactions and molecule–adsorbate interactions, is that the behavior of the one-electron states involved in bond breaking and forming is constrained fundamentally. The Pauli principle defines specific pairwise orbital interactions that must exist and will control the way the states evolve. In the case of reactions that may be classified as "exchange reactions" (such as those considered here), these restrictions can produce large barriers. We show here that it is likely that on transition metal surfaces, barriers in analogous reactions should be reduced substantially. The orbitals directly involved will seek to maximize attractive interactions while minimizing the effect of a well-defined set of repulsive interactions. Barrier heights directly reflect the degree to which the local orbital shapes may be altered to satisfy these multiple criteria at a minimum energetic cost.

(2) The presence of specific energetic interactions is determined by the form of the system wave function; the sizes of these interactions are determined by specific orbital shapes. As such, orbital symmetry arguments can present a "short-cut" to determining how the underlying energetics will evolve, since the symmetry reflects the size of the interactions. This analysis permits a more general application, however, since it is not restricted to cases where symmetry is present. As has been shown for the low-symmetry-surface processes, orbitals in the system can assume complex low-symmetry shapes in order to optimize orbital overlaps (and thus energetic interactions) for a low barrier.

(3) The partially occupied 3d orbitals in transition metal complexes and on transition metal surfaces can possess the local symmetries in the ground state that are needed to facilitate a variety of M–X + Y–Z → M–Y + X–Z exchange processes, where such processes are thermodynamically reasonable. When 3d orbitals are available on the metal atoms, local orbital symmetries prevail in the ground state of the system and a low barrier can follow via the type of interactions outlined in Figure 3. When the metal atoms comprise a metal surface, the local 3d orbitals will overlap and form a band, and the analysis must be modified to admit these neighboring interactions. In this case, the nodal patterns that evolve will be slightly more complex than for the single metal atom case, but the high density of d states makes it possible to achieve these adjustments at essentially no energetic cost.

(4) The conduction-band-surface states of both simple and transition metal surfaces, composed generally of delocalized s- and p-band electrons, usually do not possess local symmetries at a reaction site on the surface that permit the simple orbital evolution from the ground state that is outlined in Figure 3. Nevertheless, they are able in many cases to introduce the nodal character necessary to satisfy the criteria in (1) above through low-lying electronic excitations. Here, success in achieving the balance of attractive and repulsive interactions is directly related to the density of surface states for the system. At a metal surface, the density of such surface states can be high, and thus a state whose contribution is needed is accessible. In simple molecule–molecule processes involving ns or np orbitals, the discreteness of the excited-state spectrum can require prohibitively large excitation energies in order to access states of the appropriate local nodal character.

From the point of view of surface chemistry, these results suggest that there is no need to artifically distinguish between the roles played by d-band and conduction-band electrons in reactions on transition metal surfaces. Both types of states are equally capable of producing a low-energy pathway when the local density of states is high. Within this picture, barrier height is directly related to the density of both types of states at the surface. Transition metal surfaces are distinguished from simple metals in their ability to facilitate dissociative chemisorption first by this high combined density of states and, additionally, by the tendency of the d orbitals to produce low barriers via ground-state local symmetry. While it is inescapable that detailed predictions about a particular reaction on a particular metal will require extensive knowledge of the electronic structure of that surface, this fuzzy distinction between sp and d band states allows us to understand in a crude sense why there are similarities in the chemistries of transition metal groups as one proceeds between rows in the periodic table. That this should be true is not obvious when it is noted that the relative radii of valence s and d orbitals generally vary over a wide range within these groups. Similarly, these results demonstrate that adsorbate–adsorbate reactions on surfaces will be dominated by pathways in which the surface states are utilized. Pathways that involve the interaction of adsorbate orbitals that are not interacting with the surface would be expected to have barriers associated with them that are analogous to gas-phase barriers, and probably should not be viewed as competitive when making mechanistic judgments.

An area for comparison with the molecular results that remains difficult to assess is the importance of "electron counts" in determining the "allowedness" of a particular reaction (a basis for the Woodward–Hoffman rules[1]). It has been shown that an identical dependence may be derived for small molecules using a local orbital approach like that used here.[5] The analysis of these cluster calculations is greatly facilitated by the fact that only a few of the cluster orbitals actually are involved in the dissociation process. We cannot exclude the possibility, however, that on other surfaces this process might require the participation of a larger set of surface states in order to proceed with minimal activation. Since we find here that the Pauli principle restrictions forming the basis for these rules are much less important energetically, we conclude that the likelihood for classifying the surface-state participation in surface reactions according to such a rigid set of rules is correspondingly reduced. Stated simply, the one-electron states occupied by the 4s electrons even in the Ni cluster interact with one another very weakly, too weakly for this to be a significant factor in determining the activation energetics. Only those states of the cluster that possess large surface amplitude are found to participate in forming the chemisorptive bonds, suggesting that a far more important factor is that there be energetically accessible states with this character to interact with the adsorbate.

To extend these conclusions to a semiinfinite crystalline surface, it is helpful to first transform the Bloch states of the solid to a semilocalized basis using the unitary transform:

$$\phi_n(\mathbf{R}_\mu,\mathbf{r}) = \sum_{\mathbf{k}}^{BZ} \exp(-i\mathbf{k}\cdot\mathbf{R}_\mu)\Psi_n(\mathbf{k},\mathbf{r})$$

from Bloch states $\Psi_n(\mathbf{k},\mathbf{r})$ of wave vector $\mathbf{k}$ and band n to Wannier states $\phi_n(\mathbf{R}_\mu,\mathbf{r})$ localized over a compound unit cell located by the vector $\mathbf{R}_\mu$ containing more than one metal atom. If we consider, for example, a three-layer slab of two-dimensional semiinfinite extent, we may rigorously transform the Bloch solutions for this slab to be approximately localized over the 24-atom "cluster" unit cell shown in Figure 13.[22] The spectrum of Wannier states for each unit cell maps directly onto the spectrum of states for the isolated 24-atom cluster; indeed, the procedure for forming the slab Wannier states is formally analogous to bringing (or bonding) together a large number of such clusters into a periodic array and performing a Lowdin (or symmetric) orthogonalization of the delocalized states that form. The one-electron states that result greatly resemble those shown in Figure 4 except for the presence of oscillating tails that decay into the lattice. From within this

(22) In calculations employing this 24-atom unit cell as a cluster model, the results for atomic adsorption were very similar to those of the 20-atom model discussed here.

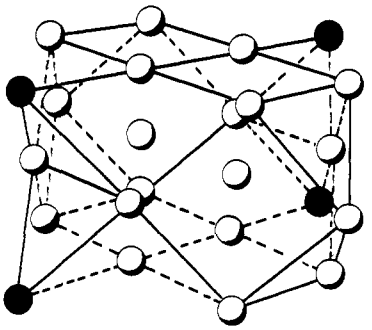

Figure 13. A 24 atom unit cell from which a three-layer fcc slab may be generated. The atoms needed to generate this "cluster" from the 20 atom cluster used in calculations here are shaded.

more localized representation, we can write the wave function for the total slab as,

$$\Psi_{slab} = \mathcal{A}\{\zeta_1\zeta_2\zeta_3\cdots\zeta_N\chi\}$$

where χ is the necessary spin function, and the ζ_i are products of the Wannier orbitals at the cell i,

$$\zeta_i = \phi_1\phi_2\phi_3\cdots\phi_n$$

Now we may approximate the interaction of a single HD molecule with the slab as the interaction of an HD molecule with one cell imbedded in the array. If we further restrict the states of the surrounding cells to be "frozen", then they serve essentially to provide only a properly screened environment for the cell of interest and establish boundary conditions for the states in that cell. From here, the analysis proceeds precisely as detailed in the previous sections, using this modified basis of occupied (and unoccupied) states in place of the cluster states used there. The validity of these approximations rests completely on the strength of interaction between the perturbed cell and the rest of the lattice.[23] If the cells are chosen to be large enough, this question becomes unimportant, as evidenced by recent chemisorption studies using clusters embedded within larger clusters.[24]

A related but less fundamental topic is the size of isolated clusters that may be adequately used to model bond-breaking processes. Much has been written about the validity of metal clusters as models for chemisorption[25] and conclusions vary. Accurate geometric and spectroscopic properties have been calculated for chemisorption systems in which as few as five metal atoms have been used as bulk models.[26] Energetic accuracy is more difficult to achieve. This difficulty may be associated with two problems: (1) the ground electronic state of the cluster may not strongly bond to the adsorbate, and (2) the excited-state spectrum of a small cluster is generally sufficiently discrete that excitations necessary to promote the cluster to a strongly bonding state may vary widely. Difficulties of this sort have been encountered in some form for clusters as large as 28 atoms.[13] When the problem being considered necessarily involves cluster excited-state character, as does the subject of this study, the difficulties are compounded and the possibility of obtaining anything more than qualitatively useful results becomes a strong function of cluster size.

Acknowledgment. The author gratefully acknowledges useful discussions with A. K. Rappé and M. L. Steigerwald during the course of this work.

Registry No. Hydrogen, 1333-74-0; nickel, 7440-02-0.

(23) An additional, but minor, concern is that occupation of the Bloch and localized states must be complete; that is, each Wannier orbital must be filled for the transformation not to affect the total energy. For the large unit cells considered here, this is not an important restriction.

(24) J. Whitten, *Phys. Rev. B*, **22**, 1910 (1981); C. Fischer, J. Whitten, and L. Burke, *Phys. Rev. Lett.*, **49**, 344 (1982).

(25) See, for example, R. Messmer in "Chemistry and Physics of Solid Surfaces", Vol. IV, R. Vanselow and R. Howe, Eds., Springer-Verlag, New York, 1982.

(26) P. Bagus and M. Seel, *Phys. Rev. B*, **23**, 2065 (1981).

π-Bond Anisotropy in the Molecular Structure of Thioacetamide

G. A. Jeffrey,*† J. R. Ruble,† and J. H. Yates

Contribution from the Department of Crystallography, University of Pittsburgh, Pittsburgh, Pennsylvania 15260, and Chemistry Department, Brookhaven National Laboratory, Upton, New York 11973. *Received June 27, 1983*

Abstract: The crystal structure of thioacetamide has been refined using single-crystal neutron diffraction data at 15 K. The structure contains two symmetry-independent molecules with different orientations of the methyl groups in space group $P2_1/c$ with a = 6.972 (3), b = 9.873 (3), c = 11.009 (4) Å, β = 99.75 (1)° at 15 K. One rotamer has close to m symmetry with planar S=C—C—N and C—C—NH_2 moieties. In the other rotamer, the methyl group is twisted 15.6° from the m symmetry orientation, and the S=C—C—N, C—C—NH_2 moieties are significantly nonplanar. There are no significant differences in the bond lengths and valence angles in the two conformers. The nonplanarity with respect to the sp^2 C atom corresponds to a pyramidalization of 0.6°. This is reproduced in direction and order of magnitude by ab initio molecular orbital calculations at the HF/3-21G and HF/3-21G(*) levels of approximation. Since a similar observation has been made for the asymmetric rotamer of acetamide, this C (sp^2) pyramidalization is believed to be an intrinsic property of the asymmetric rotamers of these molecules. In contrast, the nonplanarity of the C–NH_2 groups, also observed in these molecules, is not well reproduced by the theoretical calculations and may be due, in part, to crystal-field forces.

Introduction

The crystal structure of thioacetamide contains two crystallographically independent molecules, which are reported from an X-ray analysis[1] to have different conformations with respect to the orientation of the methyl groups. Crystal structures containing the same molecule in different conformations are uncommon, but not rareties. In the crystal structure of pinacol,[2] for example, the same molecules appear in three different conformations. What

† Research Collaborators at Brookhaven National Laboratory.

(1) Truter, M. R. *J. Chem. Soc.* **1960**, 997-1007.

(2) Jeffrey, G. A.; Robbins, A. H. *Acta Crystallogr., Sect. B* **1978**, *34*, 3817-3820.

0002-7863/84/1506-1571$01.50/0